SCISPACE formerly Typeset

Open access • Journal Article • DOI:10.1063/1.365650

Band offsets at the GaInP/GaAs heterojunction — Source link

A. Lindell, Markus Pessa, A. Salokatve, Fabio Bernardini ...+2 more authors

Published on: 01 Oct 1997 - Journal of Applied Physics (American Institute of Physics)

Topics: Band offset, Band gap, Heterojunction and Molecular beam epitaxy

Related papers:

- Band offsets at GaInP/AlGaInP(001) heterostructures lattice matched to GaAs
- Valence band offset of GaAs/GaAs0.68P0.32 multiple quantum wells
- Temperature-dependent valence band offset and band-gap energies of pseudomorphic GaAsSb on GaAs
- Strain dependence of the valence-band offset in arsenide compound heterojunctions determined by photoelectron spectroscopy
- Valance band offsets in strained GaAs 1−x P x /GaAs heterojunctions

Share this paper:

View more about this paper here: https://typeset.io/papers/band-offsets-at-the-gainp-gaas-heterojunction-3c5tr4n7fe

Band offsets at the GaInP/GaAs heterojunction

A. Lindell, M. Pessa, A. Salokatve, F. Bernardini, R. M. Nieminen et al.

Citation: J. Appl. Phys. **82**, 3374 (1997); doi: 10.1063/1.365650
View online: http://dx.doi.org/10.1063/1.365650
View Table of Contents: http://jap.aip.org/resource/1/JAPIAU/v82/i7
Published by the American Institute of Physics.

Related Articles

Polarization engineered 1-dimensional electron gas arrays
J. Appl. Phys. 111, 043715 (2012)

Impact of the misfit dislocations on two-dimensional electron gas mobility in semi-polar AlGaN/GaN heterostructures
Appl. Phys. Lett. 100, 082101 (2012)

Measurement of semiconductor surface potential using the scanning electron microscope
J. Appl. Phys. 111, 046103 (2012)

Electron mobility, Hall scattering factor, and sheet conductivity in AlGaN/AlN/GaN heterostructures
J. Appl. Phys. 110, 113713 (2011)

Reduction of the potential energy barrier and resistance at wafer-bonded n-GaAs/n-GaAs interfaces by sulfur passivation
J. Appl. Phys. 110, 104903 (2011)

Additional information on J. Appl. Phys.

Journal Homepage: http://jap.aip.org/
Journal Information: http://jap.aip.org/about/about_the_journal
Top downloads: http://jap.aip.org/features/most_downloaded
Information for Authors: http://jap.aip.org/authors

ADVERTISEMENT

Downloaded 27 Feb 2012 to 192.84.153.4. Redistribution subject to AIP license or copyright; see http://jap.aip.org/about/rights_and_permissions

Band offsets at the GaInP/GaAs heterojunction

A. Lindell
Laboratory of Applied Physics, Department of Physics, University of Jyväskylä, P.O. Box 35, 40351 Jyväskylä, Finland

M. Pessa and A. Salokatve
Tampere University of Technology, P.O. Box 692, 33101 Tampere, Finland

F. Bernardini and R. M. Nieminen
Laboratory of Physics, Helsinki University of Technology, 02150 Espoo, Finland

M. Paalanen
Low Temperature Laboratory, Helsinki University of Technology, 02150 Espoo, Finland

(Received 11 November 1996; accepted for publication 24 June 1997)

We have measured current–voltage curves and the temperature dependence of the zero bias conductance for a *p*-type Be-doped GaInP/GaAs heterojunction grown by the molecular beam epitaxy method. We have determined the valence band offset ΔE_v from both measurements and find it to be 310 meV within 5% of accuracy. Similarly, we find for an *n*-type Si-doped sample that the conduction band offset ΔE_C is 95 meV. First-principles calculations have been carried out for the atomic and electronic structures of the interfaces. For the thermodynamically favored interfaces, the valence band offset is found not to be sensitive to atomic relaxations at the interface. The calculated values are in good agreement with the experiments. © *1997 American Institute of Physics.* [S0021-8979(97)00519-7]

I. INTRODUCTION

Lattice-matched GaInP/GaAs heterojunctions are widely considered for applications such as *p*-channel field-effect transistors, heterojunction bipolar transistors, visible heterostructure lasers, and high efficiency light-emitting diodes.[1] For these applications, GaInP/GaAs heterojunctions have many advantages, for example low interface recombination velocities, high doping capability without creating deep levels, less oxidation, and large valence band offset ΔE_v, in comparison with commonly used AlGaAs/GaAs heterojunctions. A large ΔE_v reduces leak currents in transistor applications. In heterostructure semiconductor lasers, the carriers are confined in the active region between two heterojunction potential barriers. This confinement enhances stimulated emission and thus reduces the threshold current density needed to create a laser beam. The threshold current increases rapidly with increasing temperature. Therefore knowledge of the conduction and valence band offsets at the interface is important while designing hot electron, microwave, and digital applications of the structures. However, the offsets of the GaAs/GaInP heterojunction are poorly known, as the reported values of the conduction band offset ΔE_C range from 30 to 390 meV.[2] The wide distribution of measured values may be due to the differences in the samples or in the measuring techniques themselves. We have measured both *p*-*p* and *n*-*n* type heterojunctions individually, in order to obtain independent values for both the valence band and the conduction band offsets. This also allows us to check if the two offsets add up to the energy gap difference ΔE_g. This value is known to be 0.517 eV at room temperature for GaInP and GaAs.[3] Furthermore, we have measured both current–voltage (I–V) curves and the temperature dependence of the zero bias conductance for the same Be-doped *p*-*p*-GaInP/GaAs sample, in order to obtain the valence band offset by two independent methods. This allows us to check the reliability of the methods used.

We also report *ab initio* calculations of the band offsets, based on structural optimizations of the relevant interfaces. The calculations are based on the plane-wave pseudopotential methods. The results for the valence band offset agree well with the experiments.

II. EXPERIMENTAL SETUP

The GaAs/GaInP layers were grown by solid source molecular beam epitaxy on epitaxy-ready GaAs(100) substrates. The structures can be seen in Fig. 1. Fluxes for arsenic and phosphorus were produced by two valved cracker cells, where the cracking zones were operated at 920 °C. Therefore the majority of the group-V molecular species were dimers As_2 and P_2. The dopants were Be and Si for *p*- and *n*-type materials, respectively. The substrate temperature was monitored with an infra-red pyrometer.

The uniformly doped GaAs buffer layers were grown at 590 °C. The growth was interrupted at the lower GaAs/GaInP heterointerface for 2 mins during which the growth temperature was ramped down to 500 °C. When the temperature reached 520 °C, the phosphorus flux was switched on and the arsenic flux was switched off, and the growth of GaInP was commenced. The GaInP layer was doped uniformly except within 500 Å distance from the upper GaInP/GaAs interface, where doping of the GaInP layer was gradually increased to the same level as that in the top GaAs contact layer. This was done in order to make the upper heterointerface highly conducting and ohmic compared to the lower heterointerface. The top GaAs layer was highly doped in order to facilitate good ohmic contacts to it.

 0021-8979/97/82(7)/3374/7/$10.00 © 1997 American Institute of Physics

Downloaded 27 Feb 2012 to 192.84.153.4. Redistribution subject to AIP license or copyright; see http://jap.aip.org/about/rights_and_permissions

p GaAs 500 Å 5×10^{19} /cm^3
p GaInP 5000 Å 2.5×10^{16} /cm^3
p GaAs 4000 Å 1.0×10^{18} /cm^3
p GaAs substrate (100) 340 μm 1.5×10^{19} /cm^3

n GaAs 500 Å 5×10^{18} /cm^3
n GaAs 5000 Å 1.0×10^{18} /cm^3
n GaInP 500 Å 10^{15}-10^{18} /cm^3
n GaInP 5000 Å $<10^{15}$ /cm^3
n GaAs 3000 Å 1.0×10^{18} /cm^3
n GaAs substrate (100)

FIG. 1. Measured structures.

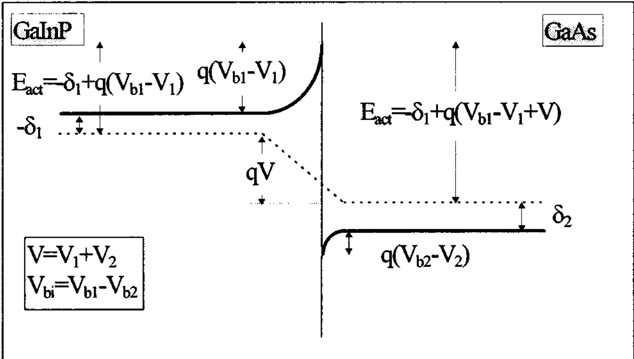

FIG. 2. Energy band diagram for an abrupt n-GaAs/n-GaInP heterojunction.

The contact patterns on the semiconductor surface were introduced by a conventional photolithography process. Exposure masks for AZ 1470 photoresist were made by electron beam lithography using scanning electron microscope.

A nonalloyed ohmic contact was produced on a p-type sample by first evaporating 250-Å-thick layer of titanium on a GaAs contact layer. To prevent the diffusion of gold into the interface titanium, a 250-Å-thick layer of platinum was evaporated on the titanium before a more than 500-Å-thick gold overcoat layer.

An alloyed contact was used on an n-type sample. A 200 Å layer of nickel was used to improve the adherence of the contact to the GaAs surface. To achieve an eutectic gold-germanium alloy, 50 Å of gold was first evaporated on the nickel layer. It was followed by a 250-Å-thick layer of germanium, and finally another 450-Å-thick layer of gold was evaporated. The alloying of n-type contacts was performed by a self-made alloying oven filled with a gas mixture of 22% hydrogen and 78% of nitrogen. The alloying temperature and time were optimized to be 450 °C and 1 min for this oven.

To prevent the lateral current flow, the semiconductor layers above the heterojunction were removed around the contact pads by wet etching. A contact pad itself was used as an etching mask for this mesa hill. An etching solution of citric acid, hydrogen peroxide, and water was used.[4]

After contacting and mesa etching, the samples were cooled close to liquid nitrogen temperature and then heated up to well above room temperature at a slow rate of 1 °C/min by scanning the set point of a temperature controller. The conductance at zero bias was measured by a four-wire method and lock-in technique. A calibrated resistor was used to obtain the temperature simultaneously.

The I–V measurements were carried out at constant temperatures by using a voltage sweep and two linear amplifiers, one for the current and the other for the voltage.

III. ANALYSIS AND RESULTS

Due to the difference in the work functions of the two materials, the energy bands bend near an n-n isotype heterojunction, as can be schematically seen in Fig. 2. The current through the junction can be derived from the thermionic emission theory when the temperature is such that the barrier height is larger than kT:[5]

$$J=A^*T^2e^{-(E_{\mathrm{act}}/kT)}, \tag{1}$$

where $A^*=4\pi q m_{\mathrm{eff}}k^2/h^3$ is the effective Richardson constant for thermionic emission. In the formula for A^*, m_{eff}, and q are the effective mass and the charge of the conduction band electrons. E_{act} is the activation energy for emitted electrons and equal to the barrier height measured from the Fermi level. By adding up the currents to both directions, the total current density can be expressed as

$$J=A^*T^2e^{-[\Delta E_c-(n-1)\delta_1-\delta_2-qV]/nkT}(1-e^{-qV/kT}), \tag{2}$$

where δ_1 and δ_2 are the Fermi energies calculated from the bottom of the conduction band in the neutral GaInP and GaAs, respectively. The ideality factor n describes the Schottky behavior of the junction. If n is close to unity, the junction resembles an ideal Schottky barrier between a metal and a low doped semiconductor.

When the applied bias voltage is high, $e^{-(qV/kt)}\ll 1$, and the reverse current J_R from GaAs to GaInP, i.e., the second term in the equation, can be ignored. From the first term which represents the forward current J_F, we can see that $\ln(J_F)$ is linear in V at a constant temperature and the conduction band offset ΔE_C can be obtained from the equation

$$\Delta E_c=nkT\ \ln\left(\frac{A^*T^2}{J_F}\right)+(n-1)\delta_1+\delta_2+qV. \tag{3}$$

For a high reverse voltage, $e^{-(qV/kT)}\gg 1$, and the second term in Eq. (2) dominates. The slope of the $\ln(J_R)$ versus V curve is mainly due to the Schottky barrier lowering and we get

$$\frac{\partial\ \ln(J_R)}{\partial V}=\frac{q(n-1)}{nkT}. \tag{4}$$

Thus, we can obtain the ideality factor n and the band offset ΔE_C from the measured I–V curves.

Similarly, we can measure the temperature dependence of the conductance with zero bias. Then the $\ln[(dJ/dV)/T]$ versus $1/T$ plot gives both the activation energy and the constant term A^* through Eq. (2)

Downloaded 27 Feb 2012 to 192.84.153.4. Redistribution subject to AIP license or copyright; see http://jap.aip.org/about/rights_and_permissions

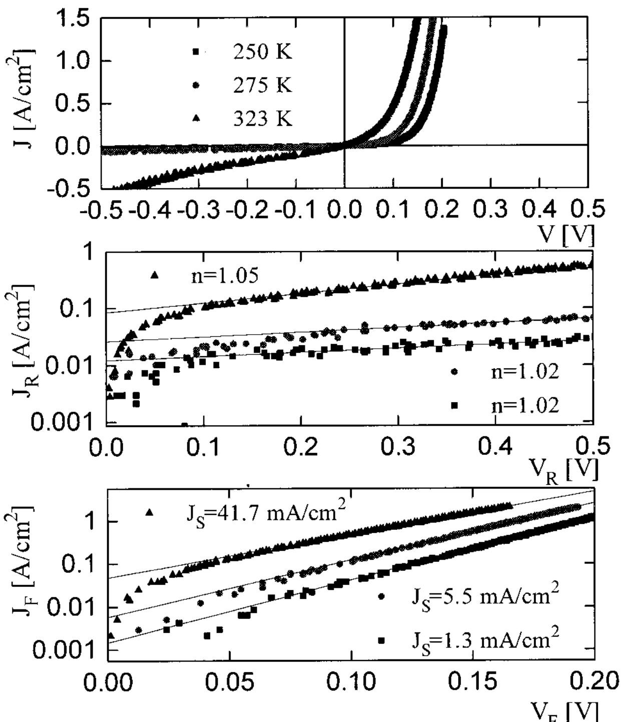

FIG. 3. Determination of valence band offset and ideality factor from I–V curves at three different temperatures for a p-GaInP/p-GaAs heterojunction.

$$\ln\left(\frac{dJ}{dV\cdot T}\right) = -\left[\frac{\Delta E_c-(n-1)\delta_1-\delta_2-qV}{nk}\right]\cdot\frac{1}{T} + \ln\left(\frac{A^*q}{k}\right). \tag{5}$$

Even though the Fermi energies δ_1 and δ_2 are strongly temperature dependent in lightly doped semiconductors, they can be estimated numerically for our doping concentrations.[6,7] The ideality factor n can be approximated as well, or it can be obtained experimentally from the I–V curves as mentioned before.

An identical analysis applies to a p-p type heterojunction, where the current carriers are positive holes in an otherwise full valence band.

Figure 3 shows measured I–V curves for a p-type sample at three different temperatures. The slopes of $\ln(J_R)$ versus V_R curves give an ideality factor close to unity as one may expect for the doping concentrations shown in Fig. 1. The intercepts of extrapolated forward currents give saturation currents J_S at zero bias. After calculating the activation energies and Fermi level corrections, all three curves give a valence band offset of (305 ± 5) meV as can be seen in Table I.

TABLE I. Determination of the valence band offset from I–V curves at four different temperatures.

T [K]	n	J_S [mA/cm^2]	E_{act} [meV]	$(n-1)\delta_1 + \delta_2$ [meV]	ΔE_V [meV]
250	1.02	1.3	346	44	302
275	1.02	5.5	350	49	301
300	1.04	14.0	369	65	304
323	1.05	41.7	373	68	305

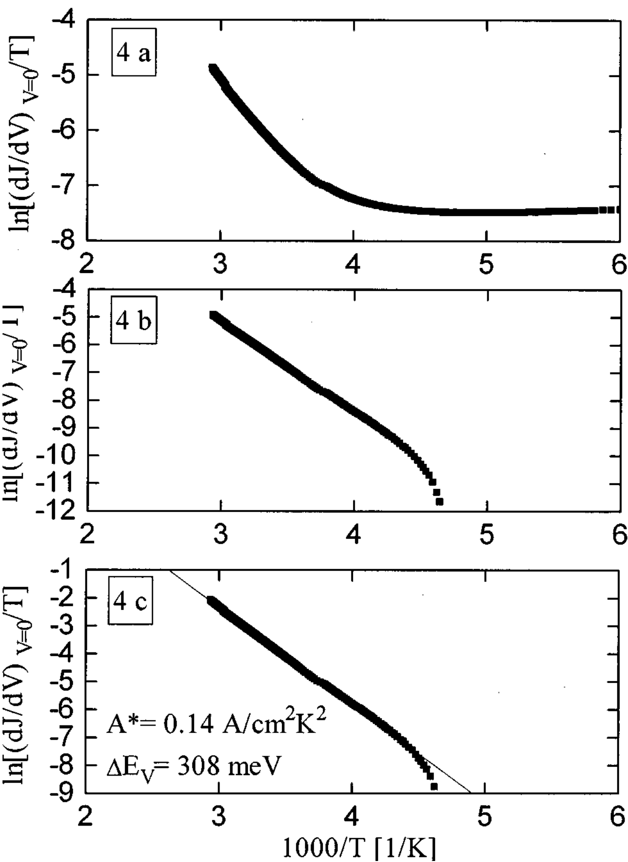

FIG. 4. Determination of valence band offset by zero bias conductance vs temperature measurements for the p-GaInP/p-GaAs heterojunction. (a) presents measured values. In (b), quantum tunneling correction has been done. The plot in (c) is achieved after quantum tunneling and Fermi level corrections have been performed. The current contact had an area of 1 mm^2 on a 500-Å-high mesa.

Figure 4 presents the zero bias conductance measurements for the same p-type sample. At low temperatures, the

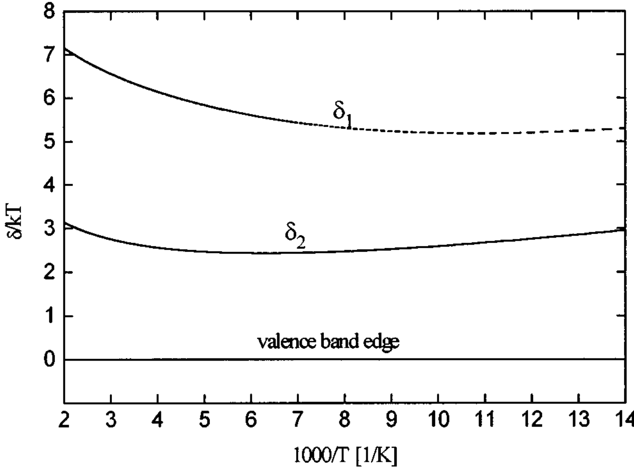

FIG. 5. Calculated values of Fermi energies δ_1 and δ_2 as a function of temperature in p-type bulk GaInP and GaAs, respectively.

Downloaded 27 Feb 2012 to 192.84.153.4. Redistribution subject to AIP license or copyright; see http://jap.aip.org/about/rights_and_permissions

TABLE II. Effective masses (Ref. 3), energies of acceptor level for beryllium dopant (Ref. 5), and doping concentrations of GaInP and GaAs in the p-type sample.

Material	m_{lh}/m_0	m_{hh}/m_0	E_A [meV]	N_A [/cm^3]
GaInP	0.145	0.660	30	2.5×10^{16}
GaAs	0.087	0.475	28	1×10^{18}

TABLE III. Effective masses (Ref. 3), energies of the donor level for silicon dopant (Ref. 5), and doping concentrations of GaInP and GaAs, respectively.

Material	m_e/m_0	E_D [meV]	N_D [/cm^3]
GaInP	0.118	11.6	1.0×10^{15}
GaAs	0.067	5.8	1.0×10^{18}

tunneling through the barrier dominates, while thermionic excitation takes place near the room temperature. For a further analysis of the thermionic current, the tunneling contribution has been subtracted from the measured data.[8] This plot can be seen in Fig. 4(b).

Figure 5 presents calculated distances of Fermi levels $\delta_1(T)$ and $\delta_2(T)$ from the top of the valence bands in GaInP (dashed curve) and GaAs (solid). The calculations were carried out at different temperatures using a procedure and formulae presented in Refs. 6 and 7. The parameters used in these calculations can be seen in Table II.

These calculated Fermi energies $\delta_1(T)$ and $\delta_2(T)$ and the ideality factor $n=1.02$, obtained experimentally from I–V measurements, were substituted into Eq. (5). This was done in order to achieve a linear plot with a slope proportional to ΔE_V and a constant term proportional to the effective Richardson constant, A^*. This plot is presented in Fig. 4(c). It gives the valence band offset of 308 meV and the effective Richardson constant of 0.14 A/cm^2 K^2. Corresponding measurements at different spots of the sample and with different contact sizes gave identical results, to within 5%.

Similarly, the plot in Fig. 6 determined from measurements of n-type samples gives the conductance band offset of 93 meV and the effective Richardson constant of 6.54×10^{-3} A/cm^2 K^2. The parameters used in calculations for Fermi level distances $\delta_1(T)$ and $\delta_2(T)$ from the bottom of the conduction bands can be seen in Table III.

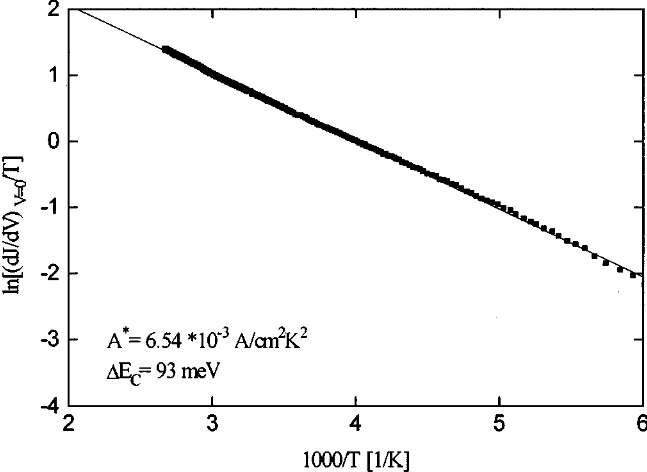

FIG. 6. Determination of conduction band offset by zero bias conductance vs temperature measurements for n-GaInP/n-GaAs heterojunction. The plot is achieved after quantum tunneling and Fermi level corrections. Current contact had an area of 0.3 mm^2 on a 5500-Å-high mesa.

IV. COMPARISON TO LASER TECHNOLOGY INTEGRATED PROGRAM SIMULATIONS

The energy band diagrams of the layered materials have also been modelled by the commercially available simulation package laser technology integrated program (LASTIP). The program is designed to simulate the operation of semiconductor lasers in two dimensions. By calibrating the program with material parameters, including the band offsets, it can be used to optimize existing lasers or to design new laser structures.

Figure 7 shows the simulated energy band diagram at 300 K for the p-type GaAs/GaInP heterojunction. The lower figure presents the valence band for an enlarged heterojunction area. The built-in voltage in GaInP, obtained from the simulation, is roughly 250 mV, and that in GaAs is approximately 20 mV. This voltage ratio gives an ideality factor of 1.08, which does not differ considerably from the experimental value of 1.04 at 300 K. The depletion layer width in

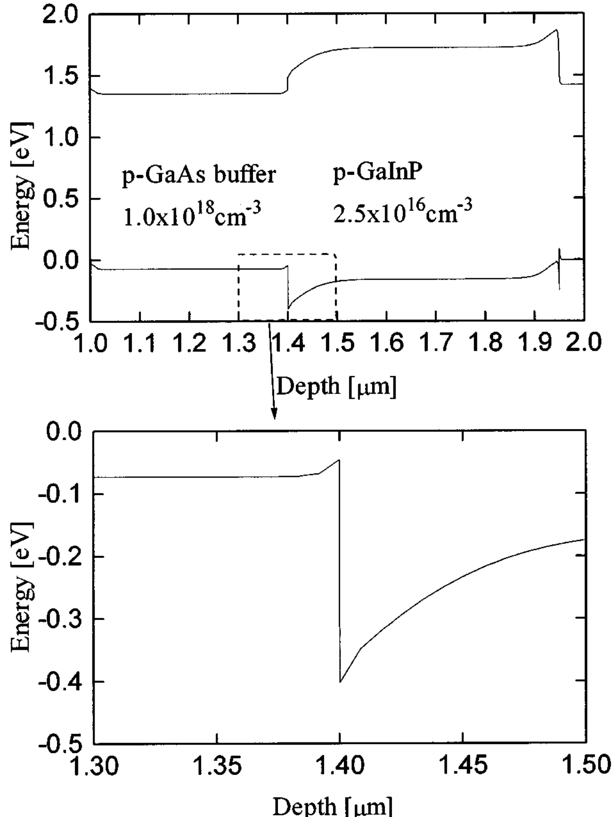

FIG. 7. Zero bias energy band diagram for a p-type GaAs/GaInP heterostructure.

Downloaded 27 Feb 2012 to 192.84.153.4. Redistribution subject to AIP license or copyright; see http://jap.aip.org/about/rights_and_permissions

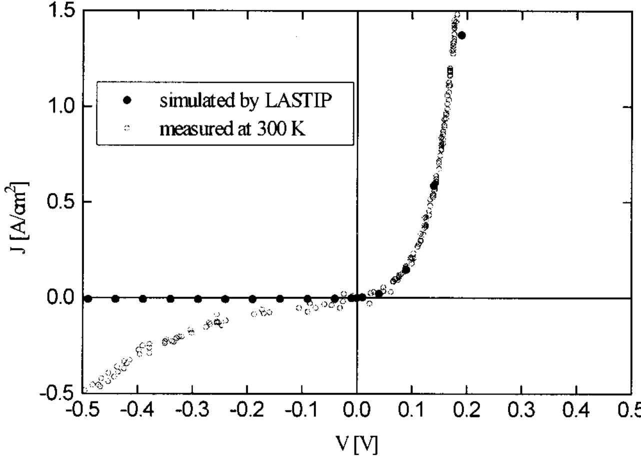

FIG. 8. I–V curves for a p-type GaAs/GaInP heterojunction at 300 K. Hollow circles represent measured values and solid ones show simulated values obtained by LASTIP program. Contact area was 1 mm^2 for both curves.

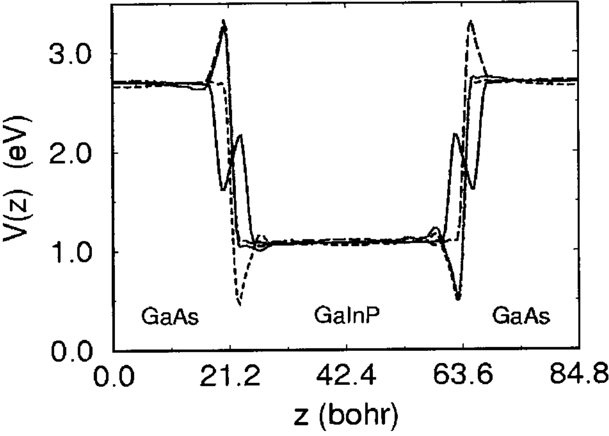

FIG. 9. Macroscopic average of the electrostatic potential through the supercell. The different lines refer to structures A (solid), B (dotted), C (long dashed), and D (dashed). A and B are the $c(2\times2)$ reconstructed (100) interfaces, containing a mixed layer of anions and cations, respectively. C and D refer to the As–Ga/In and P–Ga abrupt interfaces.

GaInP is of the order of 1 μm, while that in GaAs is much less. The difference is due to the large number of states available in GaAs.

For the n-type GaAs/GaInP heterojunction simulated energy band diagram at 300 K gives an ideality factor of about 1.1, which is slightly higher than what one would expect for the doping concentrations used. Nevertheless, the difference does not have an effect on the band offsets obtained earlier.

Figure 8 compares the simulated and measured I–V curves for the p-type sample at 300 K. The forward parts of the curves fit well together. The small difference with high forward bias voltage is obviously due to the heating of the sample by forward current. The measured reverse current is somewhat higher than the simulated one. A reason for this is probably avalanche breakdown in the edge and/or curvature regions of the junction where the field intensity is higher than in planar junction. The LASTIP program does not take into account this junction curvature effect, which increases our experimental values of the ideality factor above room temperature slightly. However, this increase with a positive temperature coefficient does not considerably affect the determined values of the band offsets.

V. *AB INITIO* CALCULATIONS OF INTERFACE STRUCTURES AND BAND OFFSETS

To gain insight into the measured band offsets, we have performed *ab initio* calculations within the density functional theory using normconserving pseudopotentials and a plane-wave basis set. The details of such calculations have been presented in a recent publication,[9] and only the main points are summarized here. A repeated-slab supercell method, with the interface of interest at its center, has been used to simulate the isolated interface by a periodic superlattice. A 12 Ryd plane-wave cutoff, sufficient to obtain an accurate description of bulk material parameters, has been used throughout the calculations. The valence-band offset ΔE_V has been calculated as outlined by Baldereschi *et al.*[10] summing two different contributions: (i) the difference ΔE_V^{BS} between the two valence-band edges measured with respect to the average electrostatic potential of each of the two bulk materials, (ii) the electrostatic potential-energy lineup across the interface ΔV_{el}. The second term is the only one in which the interface properties are involved, the other arising from the bulk properties of the constituent materials of the structure.

Even if the exact value for the band offset can not be determined by means of simple arguments, qualitative predictions can be made rather straightforwardly. In particular, the band offset between two isovalent lattice-matched semiconductors will depend only weakly on any structural property of the interface, such as the crystallographic orientation of the interface.[11] This means that the value for the band offset found for the (100) orientation of the interface is the same for every other orientation, nor does any alloying procedure at the (100) interface give a substantially different value. We have checked the dependence of the band offset on the abruptness of the interface by making self-consistent calculations for four different interface geometries, which represent limiting cases of abrupt and reconstructed interfaces of the $Ga_{0.5}In_{0.5}P$–GaAs(100) system. The interfaces considered are the two abrupt interfaces obtained bringing in contact the P-terminated alloy with the Ga-terminated GaAs and the Ga/In-terminated alloy with the As-terminated GaAs. In each case, the interface has been structurally relaxed to its equilibrium.

Among the possible reconstructions, we have considered the $c(2\times2)$ with one mixed layer containing either an anion or a cation-mixed layer. In Fig. 9, we present the distribution of the electrostatic potential after a suitable convolution (the Baldereschi average) has been carried out to filter away the bulklike contributions. The symbols A and B refer to the $c(2\times2)$ reconstruction of the (100) interface, containing a mixed layer of anions and cations, respectively, while C and D refer to the As–Ga/In and P–Ga abrupt interfaces. Regardless of the geometrical characteristics of the interface, all these four macroscopic potentials reach the same asymptotic values in the central slab region of each material. Thus no structural information is obtained from comparing the ex-

Downloaded 27 Feb 2012 to 192.84.153.4. Redistribution subject to AIP license or copyright; see http://jap.aip.org/about/rights_and_permissions

TABLE IV. Valence band offsets ΔE_v and formation energies E_f at the GaInP–GaAs(100) and AlInP–GaAs(100) interfaces (in eV). The formation energies refer to the (1×1) interface.

		A	B	C	D
GaInP/GaAs	ΔE_v	0.36	0.36	0.36	0.34
	E_f	-0.03	-0.03	$-0.43+\Delta\mu$	$-0.51-\Delta\mu$
AlInP/GaAs	ΔE_v	0.58	0.60	0.62	0.58
	E_f	0.00	0.00	$-0.48+\Delta\mu$	$0.51-\Delta\mu$

perimental value for the band offset with the outcomes of the calculations. It is indeed the case in which only an *ab initio* total energy calculation can shed light on the abrupt and reconstructed interfaces of the $Ga_{0.5}In_{0.5}P$–GaAs(100) system, otherwise inaccessible to the investigation.

The interfaces considered are the two abrupt interfaces obtained bringing in contact the P-terminated alloy with the Ga-terminated GaAs and the Ga/In-terminated alloy with the As-terminated GaAs. For each interface structure, we define and calculate the formation energy E_f dependent on the chemical potentials of the elements in question:

$$E_f=\frac{1}{2A}\left(E_{\mathrm{tot}}^{\mathrm{SL}}-\sum_i n^i\mu^i\right). \quad (6)$$

Here $E_{\mathrm{tot}}^{\mathrm{SL}}$ is the supercell total energy, n^i the number of atoms for each element, μ^i the respective chemical potential, and A the supercell cross-sectional area. In Table IV, we report the results of the calculations of the valence band offset and the formation energies for the GaInP–GaAs (100) interface. According to the above discussion, ΔE_v is the same for all the investigated interfaces except for case D in which a small deviation of 20 meV can be accounted for by the effect of the interface strain on the band offset. These numbers are in substantial agreement with the experimental values (305 meV) and the residual difference of 55 meV can probably be attributed to the effect of disorder not considered in our calculations.

For completeness, we have also calculated and tabulated in Table IV the corresponding values for the AlInP/GaAs(100) interface. Again the results for the valence band offset are in good agreement with the experimental values reported by Watanabe and Ohba.[12]

Table IV also lists the values of the interface formation energies. In the case of the abrupt interfaces, these depend on the chemical potential difference, defined as $\Delta\mu=\frac{1}{2}(\mu^{\mathrm{P}}-\mu^{\mathrm{As}})$ (equivalently for the other cases). The admitted range of this difference is determined by the equilibrium conditions for the bulk materials and the appropriate binary compounds.[13] The phase diagram is presented in Fig. 10. Depending on the chemical potentials, both abrupt interfaces are possible while the reconstructed A and B are always energetically unfavorable. Since there is no reason to suppose that more complex reconstructions should have different formation energies, we conclude that the interface geometry for the system investigated should be of the type C or D.

Summarizing this section: we have calculated valence-band offsets and formation energies for different geometrical arrangements of the $Ga_{0.5}In_{0.5}P$–GaAs(100) interface. The

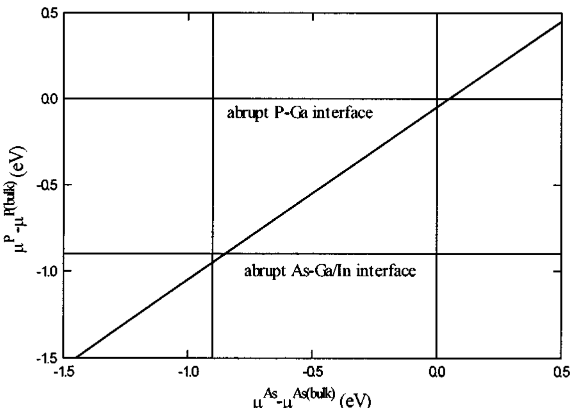

FIG. 10. Phase diagram of the energetically most favorable interfaces as a function of the chemical potentials. The chemical potentials μ^{P} and μ^{As} are referred to their corresponding bulk values.

results, in good agreement with the experimental value discussed above, show that the band offset is not sensitive to the detailed interface geometry. The total energy calculations predict that the interface is likely to be abrupt, consisting of either As–Ga/In or P–Ga depending on the relative values of the atomic chemical potentials during the interface growth.

VI. DISCUSSION

The sum of the measured band offsets at the GaAs/GaInP heterojunction is 400 meV, which is somewhat smaller than 517 meV, the difference between the band gaps of these two materials.[3] The difference may be due to the slight contamination of GaInP with arsenic during the growing process.[14] Another explanation for the deviation is that the band gap of the molecular beam epitaxy grown GaInP is less than that used in Ref. 3. If this is the case, then it is not known whether the valence or the conduction band offset is more affected.

The Schottky effect, i.e., the image force induced lowering of the barrier, can not make the difference, because this has been taken into account in the experimentally determined ideality factor. Besides, the Schottky barrier lowering is negligible in a junction between two materials with essentially the same dielectric constant.

Anyway, according to the experiment, the valence band offset is clearly larger than the conduction band offset for the GaInP/GaAs heterojunction.

The measured effective Richardson constants are smaller than the theoretical ones. The effective Richardson constant for free electrons is 120 $\mathrm{A/cm^2/K^2}$ (Ref. 5). By taking into account the effective masses of the carriers, the theoretical effective Richardson constant for a p-type GaAs is 74 $\mathrm{A/cm^2/K^2}$ and that for an n-type GaAs is 8 $\mathrm{A/cm^2/K^2}$ (Ref. 5). The respective experimental values of 0.14 and 6.54×10^{-3} $\mathrm{A/cm^2/K^2}$ were by a factor of 1000 smaller than these.

One possible reason for the low measured values of A^* is the reduced contact area by contamination of the surface or by oxidation of the contact layer dopants. Fast wet etching of

Downloaded 27 Feb 2012 to 192.84.153.4. Redistribution subject to AIP license or copyright; see http://jap.aip.org/about/rights_and_permissions

the surface by citric acid before contacting increased the values of measured Richardson constant by a factor of 10 to the values mentioned above.

The calculated values of A^* do not include the optical phonon scattering. It is possible that an electron which has enough energy to overcome the barrier scatters back due to the electron optical-phonon backscattering. Further, the Maxwellian energy distribution of electrons may be distorted because of quantum tunneling and reflection. The influence of these effects to total current density depends strongly on the electric field and the energy of the carriers.[5]

Yet, another possibility is that an alloyed contact forms spikes on GaAs despite the gapping metal between the semiconductor surface and gold layer. These spikes are narrow and sharp projections and their added up area is much less than the contact area.

Hickmott *et al.*[15] have measured an effective Richardson constant of the order of 0.1 $A/cm^2/K^2$ for an n-type doped GaAs thermionic emitter. In addition, this value decreases sharply around zero bias, reaching a minimum value of the order of 0.01 $A/cm^2/K^2$ and is close to the value obtained in our experiment.

It is risky to determine A^* from experimental data because it requires an extrapolation of a logarithmic plot on $1/T$ scale to zero, i.e., to infinite temperature. However, the effective Richardson constant, determined from the temperature dependence of the zero bias conductance, was used as a parameter in determination of the valence band offset from I–V curves. The band offsets obtained by these two independent methods fit well together. Thus, the experimentally determined A^* must be correct, as it is. The difference between calculated and experimentally determined effective Richardson constants is due to the reduction of the active contact area and reflection of carriers at the interface.

ACKNOWLEDGMENTS

This work is done in collaboration with the partners of EPIMATTER consortium and funded by the Academy of Finland.

[1] Q. Liu *et al.*, J. Appl. Phys. **77**, 1154 (1995).
[2] S. L. Feng *et al.*, Semicond. Sci. Technol. **8**, 2092 (1993).
[3] C. Jelen, S. Slivken, X. G. He, M. Razeghi, and S. Shastry, J. Vac. Sci. Technol. B **12**, 1113 (1994).
[4] M. Otsubo, T. Oda, H. Kumabe, and H. Miki, J. Electrochem. Soc. **123**, 676 (1976).
[5] S. M. Sze, *Physics of Semiconductor Devices* (Wiley, New York 1981).
[6] J. S. Blakemore, Electr. Commun. **29**, 131 (1952).
[7] D. J. Bednarczyk, Phys. Lett. A **64**, 409 (1977).
[8] L. L. Chang, Solid State Electron. **8**, 721 (1965).
[9] F. Bernardini and R. M. Nieminen, Phys. Rev. B **55**, 1718 (1997).
[10] A. Baldereschi, S. Baroni, and R. Resta, Phys. Rev. Lett. **61**, 734 (1988).
[11] G. Bratina, L. Vanzetti, L. Sorba, G. Biasiol, A. Franciosi, M. Peressi, and S. Baroni, Phys. Rev. B **50**, 11 723 (1994).
[12] M. O. Watanabe and Y. Ohba, Appl. Phys. Lett. **50**, 906 (1987).
[13] μ^{P} and μ^{As} are subject to the following boundary conditions: $\mu^{P\ bulk} \geqslant \mu^{P} \geqslant \mu^{P\ bulk} + \Delta H^{GaInP}$ and $\mu^{As\ bulk} \geqslant \mu^{As} \geqslant \mu^{As\ bulk} + \Delta H^{GaAs}$.
[14] T. Kobayashi, K. Taira, F. Nakamura, and H. Kawai, J. Appl. Phys. **65**, 4898 (1989).
[15] T. W. Hickmott, P. M. Solomon, R. Fischer, and H. Morkoc, J. Appl. Phys. **57**, 2844 (1985).

Downloaded 27 Feb 2012 to 192.84.153.4. Redistribution subject to AIP license or copyright; see http://jap.aip.org/about/rights_and_permissions